

# Temperature modulated DSC and DSC studies on the origin of double melting peaks in poly(ether ether ketone)

Chih-Lung Wei<sup>a</sup>, Ming Chen<sup>a,\*</sup>, Feng-Er Yu<sup>a,b</sup>

<sup>a</sup>*Institute of Materials Science and Engineering, National Sun Yat-Sen University, 70 Lien Hai Road, Kaohsiung 80424, Taiwan, ROC*

<sup>b</sup>*Chung Shan Institute of Science and Technology, P.O. Box 90008-20, Kaohsiung 841, Taiwan, ROC*

Received 7 May 2003; received in revised form 12 August 2003; accepted 8 October 2003

## Abstract

Crystallization kinetics and melting behavior of poly(ether ether ketone) were studied by differential scanning calorimetry (DSC) and temperature-modulated DSC (TMDSC). The isothermal crystallization was performed between 290 and 320 °C. The Avrami exponents and the level off time were determined from the Avrami analysis. The minimum induction time required for the occurrence of double melting peaks was obtained by increasing the isothermal crystallization time in steps of one minute. It was found that the level off time did not represent the delimitation of single- or double-melting peak behavior. To elucidate the behavior of double melting peaks, the samples were crystallized isothermally between 280 and 320 °C for 10 min, and then they were heated to 380 °C at 2 °C/min. From the TMDSC results, the exothermic behavior in the non-reversing curves supports the mechanism of melting–recrystallization at  $T_c \leq 310$  °C. On the other hand, no exothermic flow for  $T_c$  at 320 °C supports the mechanism of two different morphologies. As the isothermal crystallization temperature increased from 280 to 320 °C, the contribution of melting–recrystallization to the upper melting peak gradually decreased, and finally disappeared.

© 2003 Elsevier Ltd. All rights reserved.

**Keywords:** Temperature-modulated DSC (TMDSC); Double-melting behavior; PEEK

## 1. Introduction

Poly(ether ether ketone) (PEEK) is a high performance thermoplastic material with high glass transition temperature and high melting temperature [1]. It exhibits very good thermal stability [2], high chemical resistance and excellent mechanical properties [3]. These properties make PEEK an attractive matrix material in carbon fiber reinforced composites. The thermal stability experiments have indicated that PEEK is stable in nitrogen up to 400 °C, holding for 15 min [4]. After this treatment, the subsequent crystallization behavior (isothermal or non-isothermal) was independent of the prior thermal history. Detailed kinetics analyses of the isothermal and non-isothermal growth-rate data indicated that PEEK exhibited an unmistakable regime II  $\rightarrow$  III transition temperature ( $T_{II \rightarrow III}$ ) at  $296 \pm 1$  °C [5,6]. A time–temperature–transformation diagram superposed on the continuous-cooling-transformation curves could be used

to predict the regime of crystallization [7]. If the crystals were formed in regime III fashion (below 296 °C), they contained more defects and had a lower crystallinity.

Isothermal crystallization is a good way to understand the crystallization kinetics. Differential scanning calorimetry (DSC) is a major tool to study the crystallization kinetics of polymers. The well-known Avrami equation describes two crystallization stages. Velisaris and Seferis [8] proposed a model of dual crystallization mechanisms to quantitatively express the crystallization rates of PEEK in terms of a linear combination of two competing processes in parallel. The initial linear portion (slope =  $n_1$ ) corresponds to the primary crystallization process, and the secondary crystallization process (slope =  $n_2$ ) dominates after the leveling off point. Day et al. [9,10] found a lower  $n_2$  value after about 70–80% conversion from the amorphous state to the crystalline state. This ascribed the secondary crystallization to the filling within the spherulites. Hay and Kemmish [11] observed that the primary crystallization corresponded to the development of spherulites ( $n_1 = 3$ ) and contributed about 80% of the overall process, while the secondary

\* Corresponding author. Tel.: +886-7-382-4680; fax: +886-7-525-4099.  
E-mail address: [mingchen@mail.nsysu.edu.tw](mailto:mingchen@mail.nsysu.edu.tw) (M. Chen).

crystallization grew in the interlamellar space. Jonas and Legras [2] discussed why the reported  $n_1$  values ranged from 2 to 3.8 for PEEK. One reason was that DuPont DSC system wasn't in a truly isothermal condition. The other reason was the choice of the crystallization starting point, which affected the  $n_1$  value by more than 10%. Bas et al. [12] used the 'C' shape of the time–temperature–transformation diagram to describe the competition between nucleation and growth, and to explain the melting peak behavior after the melt crystallization.

The thermal treatment or thermal history of a semicrystalline polymer will be reflected in its melting behavior. Double melting peaks of PEEK were observed if the time of isothermal crystallization was long enough. The corresponding thermal history, double-melting behavior for different grades of PEEK, and their references are listed in Table 1 [11–18]. There are two major groups based on the way in which the behavior of double endothermic peaks is explained. In the first group, some researchers proposed the melt–recrystallization mechanism [19–21]. The peak at lower temperature was due to the melting of the initial crystal lamellae formed during the isothermal crystallization. When the temperature is increased, the initial crystal lamellae were melted and recrystallized to induce a higher melting peak during the heating scan. The occurrence of the second peak is due to the melting of the more perfect crystals or the thicker lamellae. The exothermic behavior of recrystallization could not be detected by conventional DSC because the extent of exothermic crystallization was less than that of endothermic melting. The second group supported the viewpoint of two different components of morphology [22]. They demonstrated that the secondary lamellae lie between the primary lamellae and both the lamellae have a widely different thickness by electron microscopy [15,23–25]. The double-melting behavior has also been studied by small angle X-ray scattering. Verma et al. [26,27] proposed thinner lamellar formed within the amorphous part by separate stacks (dual lamellar stack model) instead of infilling between the thicker lamellae (lamellar insertion model) [28–31]. Marand and Prasad [18] studied the double melting peaks of PEEK by polarized

optical microscopy. For isothermal crystallization above 300 °C, spherulitic and crystal-aggregate-like morphologies were observed. For isothermal crystallization below 300 °C, only spherulitic morphology was observed and this did not explain the two endothermic peak phenomenon. Recently, Tan et al. [32] compared the TEM morphological observations of PEEK before and after partial melting, the low-temperature melting peak is attributed to the melting of subsidiary thinner lamellae. The high-temperature one is due to the melting of the dominant thicker lamellae. TEM morphological results are consistent with small angle X-ray scattering results, which exhibit a change in the long period of the lamellar crystals before and after the partial melting process. The multiple melting behavior and morphology development during the isothermal crystallization and subsequent melting of syndiotactic polypropylene (sPP) [33] and isotactic polystyrene (iPS) [34] have also been investigated by DSC and TEM. The combination of thermal analysis and morphological results indicates that two lamellar populations are responsible for double-melting behavior.

The melting behavior of poly(phenylene sulphide) [35], poly(ethylene terephthalate) (PET) [36], poly(butylene terephthalate) [37], and poly(butylene succinate) [38] usually display triple melting peaks when scanned in a DSC. The lower and middle melting peaks were attributed to the secondary and primary crystals, respectively, formed at the crystallization temperature. The upper melting peak was associated with the crystals reorganized during the DSC scan. Temperature modulated DSC (TMDSC) is a relatively new thermal analysis instrument. It provides the information of the total heat flow, as the conventional DSC does, and the reversible signal of the heat flow derived from the heat capacity-related component. The non-reversing heat flow is obtained from the difference between the total and the reversing heat flow. The additional reversing and non-reversing signals can characterize the melting and recrystallization processes. Some laboratories also used quasi-isothermal temperature MDSC to study the reversing and non-reversing phenomena for crystallization and melting of polymers [39–42].

Table 1  
Literature review of double melting peaks and the corresponding thermal history for different grades of PEEK

Grade <sup>a</sup>	Molecular weight		Melting condition		With double melting peaks		Without double melting peaks		Ref.
	$M_n$ 10 <sup>-3</sup>	$M_w$ 10 <sup>-3</sup>	Temperature (°C)	Time (min)	Temperature (°C)	Time (min)	Temperature (°C)	Time (min)	
–	46.0	114	377	5	300	30	300	10	[11]
K200	10.8	43.0	400	5	300	1	300	sec	[13]
–	14.0	–	–	–	300	10	300	5	[14]
–	–	–	400	1	310	10	310	6	[15]
–	–	–	407	2	310	10	310	7.5	[16]
450G	–	–	–	–	310	30	350	30	[17]
K200	17.2	38.0	400	5	315	10	320	10	[12]
380G	13.5	36.0	390	3	320	50	320	30	[18]

<sup>a</sup> Stabar K200, 450G, and 380G are products of ICI.

In the present work, the isothermal crystallization of PEEK was studied by using DSC. The level off time determined from the Avrami analysis will be compared with the minimum induction time for the occurrence of the double melting peaks. From the TMDSC experiments, the melting behavior and the mechanisms of single- and double-melting peak are discussed. The results indicated that the double-melting peak was attributed to both mechanisms of two different morphologies and melting–recrystallization. The origin of double-melting peak depends on the temperature and time of isothermal crystallization.

## 2. Experimental

### 2.1. Materials

The PEEK powders, commercial-grade 150P, were obtained from Imperial Chemical Industries (ICI). The number and weight average molecular weights,  $M_n$  and  $M_w$ , were 10,300 and 26,800 g mol<sup>-1</sup>, respectively [43]. Its glass transition temperature ( $T_g$ ), melting temperature ( $T_m$ ), and equilibrium melting temperature ( $T_m^0$ ), were 143, 335 and 395 °C, respectively [44].

### 2.2. Sample preparation

The PEEK powders were sandwiched between two polyimide films and two aluminum plates, and then they were put in a modified diaphragm forming apparatus [7]. The powders were heated from room temperature to 400 °C at a heating rate of 10 °C/min and held at 400 °C for 15 min under vacuum. During the compression molding process, up to 6 kg/cm<sup>2</sup> (100 psi) of nitrogen pressure was applied. Then the samples were cooled down to room temperature at the maximum cooling rate to obtain void free, uniform thick and good quality samples for DSC study. The compressed film had a thickness of about 0.2 mm.

### 2.3. Differential scanning calorimetry (DSC)

A Perkin–Elmer Pyris 1 DSC was used to investigate the isothermal crystallization kinetics and the melting behavior of PEEK under nitrogen. Both temperature and heat flow scales were routinely calibrated with indium and zinc under a constant nitrogen flux. About 9 mg of sample was used in this study. For the isothermal crystallization case, the samples were first heated from room temperature to 400 °C at 10 °C/min and held in molten state for 15 min to obtain nuclei-free melt. They were quickly cooled at a nominal rate of 240 °C/min to the preset temperature between 290 and 320 °C. The enthalpy of crystallization exotherm was measured as a function of time, and the crystallization kinetics was analyzed by Avrami's method. To study the minimum induction time for the occurrence of the double melting peaks, the samples were treated in the same molten

condition except the isothermal crystallization time was varied from 1 to 14 min. Then they were scanned directly from the crystallization temperatures up to 380 °C at 10 °C/min.

### 2.4. Temperature modulated DSC (TMDSC)

For the TMDSC experiments, model 2910 DSC from TA Instruments (Newcastle, DE) was used to investigate the melting behavior of PEEK. The cell constant calibration was performed with an Indium standard, and the temperature calibration was obtained with Indium and Lead metals. A standard sapphire sample was used to measure the heat capacity calibration constant for the modulation study. A heating rate of 2 °C/min with a period of 60 s and a modulation amplitude of 0.318 °C was chosen based upon the recommended specifications given in the instrument manual [45]. The modulation temperature amplitude is smaller relative to the heating rate, so there is no local cooling during the scan, which is referred to as heating-only. The mathematical equation representing DSC heat flow can be expressed as [46]

$$d\theta/dt = C_p(dT/dt) + f(t, T) \quad (1)$$

where  $\theta$  is the amount of heat absorbed by the sample,  $t$ , the time,  $C_p$ , the heat capacity of the sample,  $T$ , the absolute temperature, and  $f(t, T)$ , is the function of time and temperature that govern the kinetics response of any physical or chemical transition.

Eq. (1) states that the heat flow of conventional DSC,  $d\theta/dt$ , contains two components: one depends on the heating-rate ( $dT/dt$ ), and the other is related to the absolute temperature. It shows that TMDSC could separate the total heat flow (abbreviated as T) into the heat capacity-related (reversible, as R) component and the kinetics (non-reversing, as NR) component of the heat flow. The reversible signal is excellent for quantifying the endothermic melting, while the non-reversible signal contains components of endothermic and exothermic events. To study the melting behavior, the samples were melted at 400 °C for 15 min, and then quickly cooled to the preset temperature between 280 and 320 °C for 10 min of isothermal crystallization, and then they were scanned directly from  $T_c$  up to 380 °C at 2 °C/min.

## 3. Results

### 3.1. Isothermal crystallization kinetics

The total crystallization time at temperature between 290 and 320 °C are listed in the second column of Table 2. The time increased from 3.20 min at 290 °C to 37.75 min at 320 °C. The whole exothermic peak was integrated to get the heat of crystallization, and the absolute crystallinity was calculated by dividing the heat of crystallization by 130 J/g

Table 2  
Analysis of isothermal crystallization kinetics of PEEK

Isothermal temperature (°C)	Crystallization time (min)		Crystallinity		Avrami analysis				Time <sup>a</sup> (min)
	Total	Level off	Absolute, total	Relative, level off	$n_1$	$n_2$	$R_1^2$	$R_2^2$	
290	3.20	0.59	0.37	0.95	1.50	0.52	0.996	0.999	2
295	8.50	0.81	0.38	0.91	1.53	0.40	0.992	0.997	
300	15.12	1.52	0.38	0.88	1.61	0.53	0.999	0.991	3
310	22.95	3.05	0.40	0.77	2.28	0.80	0.995	0.991	5
315	26.52	5.39	0.40	0.67	2.80	1.18	0.998	0.993	
320	37.75	7.47	0.37	0.42	2.98	1.37	0.998	0.999	12

<sup>a</sup> Minimum time for the occurrence of double melting peaks.

[44]. The results of total crystallinity are tabulated in the fourth column of Table 2. The absolute crystallinity was almost constant with values between 0.37 and 0.40 for specimens crystallized isothermally between 290 and 320 °C.

The integration over the whole peak of crystallization is expressed as  $\int_0^\infty (dH/dt)dt$ , which is the denominator of Eq. 2.

$$X_c(t) = \int_0^t \left( \frac{dH}{dt} \right) dt / \int_0^\infty \left( \frac{dH}{dt} \right) dt \quad (2)$$

The relative degree of crystallization  $[X_c(t)]$  at time  $t$  was calculated from the ratio of the partial integration area at time  $t$  and the area of whole crystallization peak. These procedures were carried using the software of the DSC system. A typical Avrami plot with  $\log[-\ln(1 - X_c(t))]$  against  $\log t$  is shown in Fig. 1 for the specimen crystallized isothermally at 300 °C. This curve has an initial linear portion corresponding to an Avrami exponent of 1.61 ( $n_1$ ). The correlation coefficient was 0.999 for this linear regression. The best fit for the leveling off portion provides the value of the second Avrami exponent ( $n_2$ ). The  $n_2$  value and the correlation coefficient are 0.53 and 0.991, respectively. The leveling off point was defined as the

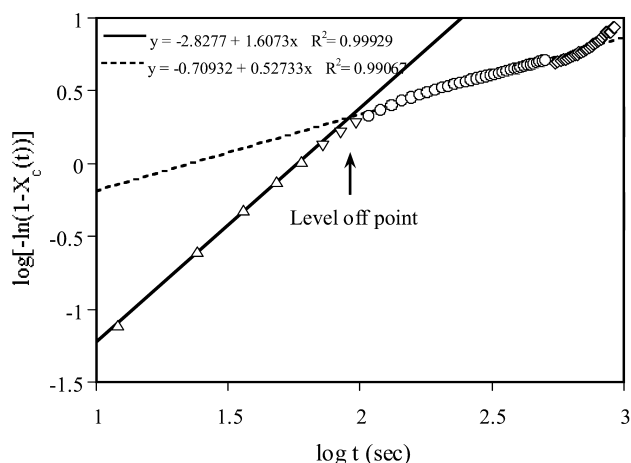


Fig. 1. Plot of  $\log[-\ln(1 - X_c(t))]$  vs.  $\log t$  for PEEK crystallized isothermally at 300 °C.

intersection point of these two linear regression lines. It was found at 1.52 min with a relative crystallinity of 0.88 for specimen crystallized isothermally at 300 °C. These results are listed in the row of 300 °C in Table 2. The total crystallization time, the absolute crystallinity of complete crystallization, the crystallization time and the relative crystallinity at the leveling off point, the Avrami exponents ( $n_1$  and  $n_2$ ) and the correlation coefficients ( $R_1^2$  and  $R_2^2$ ) are summarized in columns of 2, 4, 3, 5, and 6–9 of Table 2 for specimens crystallized isothermally between 290 and 320 °C. All of the correlation coefficients above 0.991 represent an extremely good fit of the Avrami equation.

The DSC thermograms at a heating rate of 10 °C/min for specimens isothermally crystallized at 290, 300, 310 and 320 °C for different time durations are plotted in Fig. 2a–d, respectively. In Fig. 2a, single endothermic melting peak or double melting peaks are shown for specimens crystallized at 290 °C isothermally for 1 or  $\geq 2$  min, respectively. A similar phenomenon was observed at other crystallization temperatures as well. The minimum induction time for the occurrence of double melting peaks are 3, 5, and 12 min, respectively, for crystallization isothermally at 300, 310, and 320 °C (Fig. 2b–d). These induction times are also listed in the last column of Table 2. The time required for the occurrence of double melting peaks increases with increasing the crystallization temperature in this nucleation control range. There is only one melting peak in short crystallization time. The results indicated that the upper melting peak appeared first, and then the lower melting peak occurred at a longer crystallization time. In Fig. 2, the temperature of the lower melting peak gradually shifts to a high temperature position with increasing crystallization time due to the improvement in the crystal structure, however, the peak location of the upper melting peak remains constant over the range of crystallization time examined.

### 3.2. Melting behavior studied by TMDSC

Fig. 3 shows the typical double melting peaks in the total curve of TMDSC (symbol as T) for the specimen isothermally crystallized at 280 °C for 10 min, but the

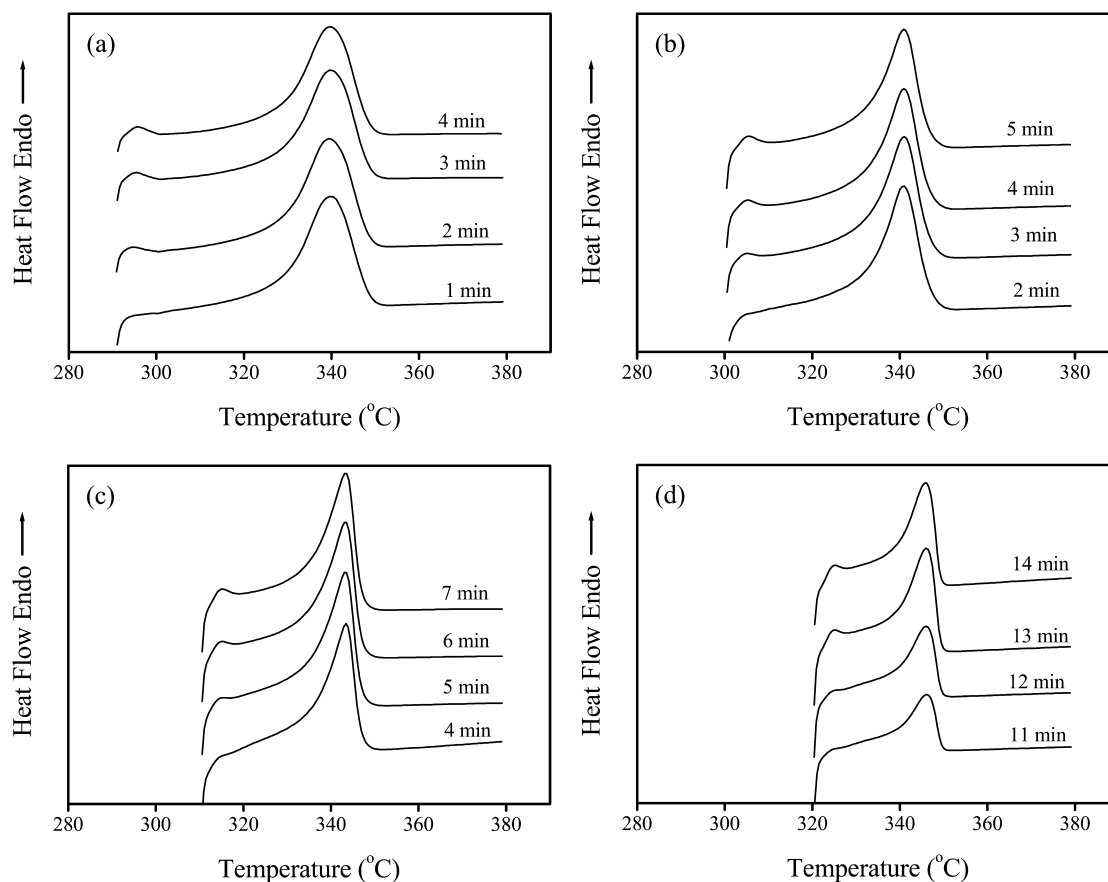


Fig. 2. DSC thermograms at a heating rate of 10 °C/min for PEEK specimens after melting at 400 °C for 15 min and then crystallizing isothermally at (a) 290, (b) 300, (c) 310, and (d) 320 °C for various time.

exothermic recrystallization is not detected. A strong exothermic phenomenon can be found in the NR curve. The exothermic process starts from 289 °C and extends up to 346 °C, which is located between two small endothermic melting peaks. The maximum point of the exothermic peak in the NR curve is at about 335 °C. In the reversing curve (symbol as R), the melting process starts at about 283 °C, and the amount of endotherm increases slowly, finally

reaching a peak at about 344 °C. In Fig. 4, the exothermic amount in the NR curve for the specimen crystallized at 300 °C is less than that for the specimen crystallized at 290 °C. Both the exothermic processes extend to about 345 °C that is close to the peak of the reversing curve. Upon increasing  $T_c$  from 280 to 310 °C (Figs. 3–5), the exothermic amount in the NR curve becomes smaller and smaller. Finally for the specimen crystallized at 320 °C,

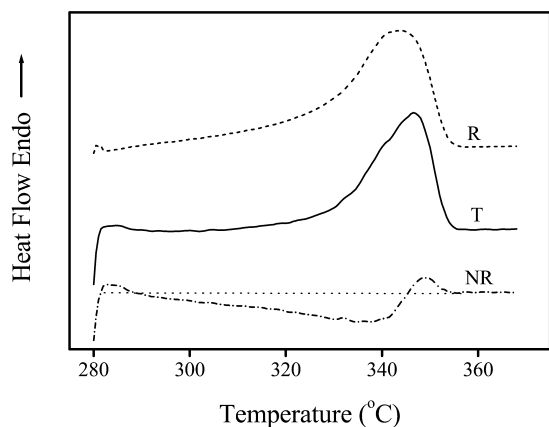


Fig. 3. TMDSC thermogram at a heating rate of 2 °C/min for PEEK specimen after melting at 400 °C for 15 min and then crystallizing isothermally at 280 °C for 10 min.

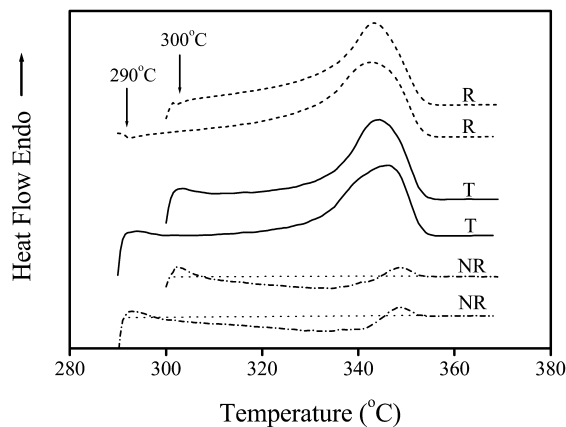


Fig. 4. TMDSC thermograms at a heating rate of 2 °C/min for PEEK specimens after melting at 400 °C for 15 min and then crystallizing isothermally at 290 and 300 °C, respectively, for 10 min.



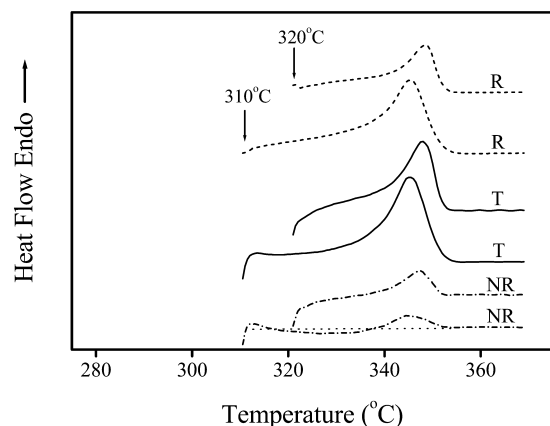


Fig. 5. TMDSC thermograms at a heating rate of 2 °C/min for PEEK specimens after melting at 400 °C for 15 min and then crystallizing isothermally at 310 and 320 °C, respectively, for 10 min.

only a single melting peak is observed in the NR curve, and the exothermic phenomenon is not detected, as shown in Fig. 5.

The TMDSC data shown in Figs. 3–5 are tabulated in Table 3. The temperatures of the upper melting peak in the total and the reversing curves are listed in the second and third columns. In the reversing curves, the peaks are broad for  $T_c$  at 280 and 290 °C. Therefore, the temperature of the upper melting peak can be considered as constant ( $343.3 \pm 0.6$  °C) for the specimens crystallized between 280 and 300 °C, then it increases continuously from 343.3 to 348.4 °C as  $T_c$  increases from 300 to 320 °C. In the total curves, the upper melting peaks for the specimens isothermally crystallized at 280 and 290 °C remained at almost the same temperature ( $346.4 \pm 0.2$  °C). However, the temperature of the melting peak decreased 2.0 °C at 300 °C, and then increased to 345.2 and 347.8 °C at 310 and 320 °C, respectively. The difference in the melting temperature between the total and the reversing curves,  $\Delta T$ , is listed in the fourth column of Table 3. The difference is negative in the case of 310 and 320 °C, i.e. the melting

temperature of the upper peak in the total curve is less than that in the reversing curve.

In Figs. 3–5, the area underneath the melting peaks was integrated for the total and the reversing curves, and the absolute crystallinity was calculated by dividing the heat of fusion by 130 J/g [44]. The crystallinities in the total and the reversing curves are tabulated in the fifth and sixth columns, respectively. The crystallinity from the total curve is between 33.4 and 36.9% for the specimens crystallized isothermally between 280 and 310 °C for 10 min. It drops to 21.8% at 320 °C. On the other hand, the crystallinity from the reversing curve decreases from 48.6 to 35.0% at  $T_c$  between 280 and 310 °C. It is only 18.3% at 320 °C. The difference of the absolute crystallinity between the reversing and the total curves,  $\Delta X_c$ , is listed in the last column of Table 3. The difference is about 14% at 280 and 290 °C, but it is –3.4% at 320 °C. Therefore, the amount of exotherm in the reversing curve is higher at  $T_c$  between 280 and 310 °C, and becomes less at 320 °C.

## 4. Discussion

### 4.1. Avrami exponents

In Table 2, the  $n_1$  values for the specimens crystallized isothermally at 320 and 315 °C were 2.98 and 2.80, respectively. It suggests that the initial stage of crystallization is a heterogeneous nucleation with three-dimensional growth. In the previous studies [4,5], the thermal history of PEEK could be erased without decomposition by holding it at 400 °C for 15 min, i.e. there was no nuclei left after this molten condition. However, the rate of homogeneous nucleation increased rapidly below 320 °C [6,7]. There were some nuclei formed during the cooling from 400 °C to 320 or 315 °C. The  $n_1$  value at 315 °C (2.80) is less than the theoretical value of 3 because the overall crystallization rate is faster than that at 320 °C. The  $n_2$  values in the latter stage of crystallization were 1.37 and 1.18, respectively, because the secondary crystals grew in a heterogeneous condition between the crystal lamellae with a geometrical dimension much less than 2.

In the case of 290 and 295 °C, the  $n_1$  values were 1.50 and 1.53. It is supposed to be heterogeneous nucleation, and diffusion-controlled growth with a geometrical dimension of three (case I), or interface-controlled growth with a geometrical dimension between one and two (case II). It is well known that the viscosity of PEEK is very high even in the molten state [4] which supports case I. The major reason for case II is that the cooling rate was not fast enough to cool the specimen to  $T_c$  without crystallization. It is reasonable to suspect that the lower the temperature for the isothermal crystallization, the higher the possibility for the occurrence of crystallization. In addition, the geometrical dimension of thin specimen in the DSC pan is between two and three instead of only three. In the latter stage of crystallization, the

Table 3

Melting temperatures and absolute crystallinity determined from the total and the reversible TMDSC thermograms for PEEK specimens after melting at 400 °C for 15 min followed by isothermal crystallization at  $T_c$  for 10 min

$T_c$ (°C)	Upper melting temperature (°C)			Absolute crystallinity (%)		
	Total	Reversing	$\Delta T^a$	Total	Reversing	$\Delta X_c^b$
280	346.54	343.96	2.58	34.22	48.64	14.42
290	346.27	342.73	3.54	33.41	46.88	13.47
300	344.40	343.33	1.07	36.88	43.08	6.20
310	345.19	345.31	–0.12	34.89	35.02	0.13
320	347.82	348.43	–0.61	21.76	18.32	–3.44

<sup>a</sup> Difference in melting peak between the total and the reversing signals.

<sup>b</sup> Difference in absolute crystallinity between the reversing and the total signals.

$n_2$  values (0.52 and 0.40) at 290 and 295 °C corresponded to a rod-shaped (or one dimension) growth with diffusion-control among the existing crystals. The  $n_1$  and  $n_2$  values for  $T_c$  at 300 or 310 °C lie between the above-mentioned two conditions.

#### 4.2. Time for the occurrence of double melting peaks

In Table 2, the time for complete crystallization detected by DSC, the time at the level off point determined from the Avrami analysis, and the minimum time for the occurrence of double melting peaks gradually increased with an increase in  $T_c$  from 290 to 320 °C. The reason is that the overall crystallization (both nucleation and crystal growth) rate is slower at higher  $T_c$  with a lower supercooling. At a  $T_c$  of 290 °C, the minimum time for the occurrence of double melting peaks was 2 min that is longer than the level off time of 0.59 min. Similar results are obtained for  $T_c$  at 300, 310 and 320 °C. This result is not consistent with that reported by Velisaris, Seferis [8], Ko and Woo [14] who proposed that only the primary crystals grew before the level off time, and the secondary crystals would emerge in parallel with the still-growing primary crystals after the level off time.

Deslandes et al. [47] suggested that the secondary process took place after the spherulites have impinged on each other. It is well known that the maximum square packing for sphere is 0.785 [48]. In the following discussion, assume that the percentage of relative crystallinity is the same as the volume fraction of crystals. As we know, regime II  $\rightarrow$  III transition occurred around 296 °C, and the perfection (or absolute crystallinity) of a spherulite increased with increasing  $T_c$ . This assumption will not change the deduction. First, for  $T_c$  at 290 and 300 °C, the level off crystallinities were 0.95 and 0.88, respectively. It indicated that the level off point was located after the primary crystals had impinged, and the secondary crystals were grown after the maximum packing at this lower temperature, 290 or 300 °C. The minimum induction time for the occurrence of double melting peaks (2 min) was close to the level off time (0.59 min) because the growth rate was faster, and the time required for complete crystallization was shorter at lower  $T_c$ . Next, let us discuss the highest  $T_c$ , in which the level off crystallinity at 320 °C was 0.42 that is much less than 0.785. It indicated that most of the primary crystals did not impinge each other at the level off time, and more time was required to achieve the maximum packing. The secondary crystals might already grow within the primary crystal lamellae due to the much slower growth and nucleation rates at 320 °C [5]. The phenomenon of secondary crystallization might be too weak to be detected due to the slower growth rate. It made the minimum induction time for the occurrence of double melting peaks (12 min) to be longer than the level off time (7.47 min) at  $T_c = 320$  °C. The difference between these two times increased with  $T_c$  (compare the last and the third

columns in Table 2). For  $T_c$  at 310 °C the level off crystallinity was 0.77, where the primary crystals would impinge each other and the secondary crystallization process would start simultaneously. However, the minimum induction time (5 min) was still longer than the level off time (3.05 min) in the case of 310 °C.

From the difference between the total and the level off crystallization time, it is clear that the secondary crystallization process after the level off point was very slow and time consuming. It can be explained based on the fact that the secondary crystallization was impeded by the existing spherulites, which in turn led to a much slower crystallization rate. From the above discussion, the minimum induction time was always longer than the level off time, which cannot be used as the delimitation for the occurrence of single or double melting peaks. The difference between the minimum induction time and the level off time increases with increasing the temperature for isothermal crystallization.

Now, let us discuss why the time required for the occurrence of double melting peaks at 300 °C in the literature [13] (1 min, as shown in the second row of Table 1) is shorter than the present result (3 min, see the third row of Table 2). The melting condition for Stabar K200 was at 400 °C for 5 min, which is shorter than the time (15 min) required to erase the thermal history. Therefore, there were some unmelted nuclei left, and they made the primary crystals and the secondary crystals (lower melting peak) occur in a shorter time. This could be the reason why the induction time at 300 °C is shorter in the literature. In the other two cases (first and third rows of Table 1), higher molecular weight increases the viscosity resulting in a longer induction time for the occurrence of double melting peaks.

For  $T_c$  at 320 °C, the reported time for the occurrence of double melting peaks (50 min) from the literature [18] (see the last row of Table 1) was longer when compared to the 12 min determined in this study (as shown in Table 2). The melting condition for PEEK 150P was 400 °C for 15 min [5]. The molecular weight of PEEK 380G is higher than that of PEEK 150P. The equilibrium melting temperature is also supposed to increase upon increasing the molecular weight. The melting PEEK 380G at 390 °C for 3 min was not high and long enough to erase the thermal history. It is suspected that there was a large amount of crystal residues left. The high molecular weight materials have a higher degree of supercooling and nucleation rate than the low molecular weight materials at higher  $T_c$ . However, the high molecular weight materials had a relatively high viscosity, and a relatively slow growth rate at lower  $T_c$ . It may be one of the reasons that made the occurrence of double melting peaks at such longer time.

In the case of 310 °C, the minimum time required for the appearance of double melting peaks was 5 min in this study, as shown in the fourth row of Table 2. The corresponding time for crystallization temperature at 310 °C was 30 min as

listed in the sixth row of Table 1. The molecular weight of PEEK 450G is higher than that of 380G, which is in turn higher than that of 150P. These results indicated that the melting viscosity was more important than the degree of supercooling to dominate the growth of secondary crystals [11].

#### 4.3. Melting behavior and mechanisms of double melting peaks

For the specimen isothermally crystallized at 320 °C for 10 min, this time of isothermal crystallization was less than the minimum time for the occurrence of double melting peaks (12 min, see the last column of Table 2). As shown in Fig. 5, only a single melting peak in all of the TMDSC curves was consistent with the results of isothermal crystallization kinetics (Section 3.1). There is no low melting peak and recrystallization in the NR curve. This indicated that the single melting peak in the total or reversing curve was due to the melting of primary crystals. The insufficient time for isothermal crystallization at 320 °C led to the absolute crystallinity drop to ~20%, as shown in the fifth and sixth columns of Table 3. Although the crystallization is not complete, the melting temperature is still the highest because the primary crystals are formed at 320 °C that is much higher than  $T_{II \rightarrow III}$ , 296 °C [5,6]. The increase of the melting temperature in the reversing curve could indicate a genuine increase in the perfection of primary crystals. Recently, Liu et al. [34] proposed that the high-temperature melting peak for isotactic polystyrene sample is due to the melting of dominant thicker lamellae by TEM studies, and to some less extent, the melting of a recrystallized population from the melted defect lamellae during the heating process in DSC.

Isothermal crystallization was performed in the temperature range between 280 and 320 °C, which is either below or above  $T_{II \rightarrow III}$ . From the NR curves in Figs. 3–5, as  $T_c$  decreases, the lower melting temperature of the secondary crystals also decreases, and more time is allowed to recrystallize during the heating scan at a rate of 2 °C/min. The corresponding exothermic area is also increased, especially for the specimen isothermally crystallized at a temperature of regime III. The  $\Delta X_c$  given in the last column of Table 3 is related to the amount of exothermic peak in the NR curves. Its value is about 14% at  $T_c < T_{II \rightarrow III}$ , and then drops to 6% at 300 °C, and becomes zero or negative at  $T_c > T_{II \rightarrow III}$ . It indicated that the contribution of recrystallization gradually decreased upon  $T_c$  increasing from 280 to 310 °C, finally disappeared completely at a  $T_c$  of 320 °C. The exothermic behavior in the NR curves supports the mechanism of melting–recrystallization at  $T_c \leq 310$  °C. On the other hand, no exothermic flow and double melting peaks for the specimens isothermally crystallized at 320 °C for 60 min [49] support the mechanism of two different morphologies. In this study, no exothermic flow and single

upper melting peak are observed for the specimens isothermally crystallized at 320 °C for 10 min.

In Table 3, the variation of upper melting temperature in the total curve with  $T_c$  could be explained from the TMDSC thermograms, as shown in Figs. 3–5. According to the study of Sauer et al. [50], the TMDSC data prove that the ‘low endotherm’—routinely detected by the standard DSC a few degrees above isothermal annealing temperature—is not a true ‘low endotherm’, but is a superposition of early melting of secondary crystals with almost simultaneous exothermic recrystallization. The upper melting temperature of the total curve is not a true upper melting temperature in this study, too. At  $T_c \leq 300$  °C, the tail of the exothermic flow in the NR curve overlaps with the peak in the reversing curve, the shift of the upper melting peak to a higher temperature in the total curve depends on the amount of overlapping. This gives rise to the melting temperature in the total curve and  $\Delta T$  at 300 °C to be smaller than those at 280 or 290 °C, as shown in the second and fourth columns of Table 3. For  $T_c$  at 310 °C, the exothermic flow is not distinct in the NR curve and extends up to 338 °C, which is 7 °C less than the peak temperature of the reversing curve. Therefore, the upper melting temperature increases to 345.2 °C for  $T_c$  at 310 °C ( $> T_{II \rightarrow III}$ ). As  $T_c$  was increased up to 310 and 320 °C, the crystals were formed in regime II. The increase of the upper melting temperature in the reversing curve could indicate a genuine increase in the perfection of primary crystals. This melting behavior again supports the mechanism of two different morphologies.

Day et al. [9] proposed that the double melting peaks were always formed for PEEK specimens isothermally crystallized or annealed below 300 °C in an ordinary DSC run (scan at 10 or 20 °C/min). Their upper melting temperatures remained constant. It was explained based on the fact that recrystallization occurred during the DSC run, and the recrystallization was a fast process in regime III. This statement is consistent with the results of TMDSC at a heating rate of 2 °C/min for  $T_c$  at 280 and 290 °C in this study. This discussion supports the mechanism of melting–recrystallization at  $T_c \leq 300$  °C.

Ko and Woo [14] proposed that polymer chains were folded into thin crystallization lamellae at low temperature. They were unstable with time and temperature. As the polymer was heated at a slower scanning rate, the thin crystallites would be gradually reorganized into thicker lamellae. The thickened lamellae would contribute a small extent to the formation of the upper melting peak during the scanning. From Figs. 3–5 and Table 3 in this study, the endothermic melting in the reversing curve dominated the double melting peaks of two morphologies, and the upper endothermic melting in the NR curve was small and covered within the peak of the reversing curve. As  $T_c$  increased from 280 to 310 °C, the exothermic amount in the NR curve became less and less, and its contribution to the endothermic curves gradually decreased. Finally, the phenomenon of melting–recrystallization–remelting disappeared comple-



tely for  $T_c$  at 320 °C. From the comparison of PEEK with PET and poly(ethylene naphthalate) (PEN) in the literatures [50–52], the apparent reorganization phenomena were induced after the melting of secondary/imperfect crystals in the NR curves. The melting peak of perfect crystals by the reorganization process appeared behind the melting peak of primary crystals for PET and PEN samples in the reversing curves, however, both melting peaks always merge together to form one single melting peak for PEEK samples. This is due to the fact that the upper melting peak for PEEK sample was mainly attributed to the primary crystal, while that for PET and PEN samples were dominated by the perfect crystal due to the reorganization process. Therefore, it was the double melting peaks, not the triple melting peaks in the total curve for PEEK sample.

## 5. Conclusion

The isothermal crystallization kinetics of PEEK was analyzed between 290 and 320 °C by Avrami equation. The corresponding Avrami constants  $n_1$  increased from 1.50 to 2.98, and  $n_2$  changed from 0.52 to 1.37. It was found that the minimum time required for the occurrence of double melting peaks was always longer than the level off time, which cannot be used as the delimitation for the occurrence of single or double melting peaks.

From the TMDSC results of crystallized samples between 280 and 310 °C, the exothermic behavior in the NR curves supports the mechanism of melting–recrystallization at  $T_c \leq 310$  °C. On the other hand, no exothermic flow for  $T_c$  at 320 °C supports the mechanism of two different morphologies. As the isothermal crystallization temperature increased from 280 to 310 °C, the contribution of melting–recrystallization to the upper melting peak gradually decreased. In the case of 320 °C, the origin of single melting peak corresponded to the primary crystals.

## Acknowledgements

The authors acknowledge the financial support of the National Science Council of Taiwan, ROC, through Grant NSC 89-2216-E-110-027.

## References

- [1] Attwood TE, Dawson PC, Freeman JL, Hoy LRJ, Rose JB, Staniland PA. *Polymer* 1981;22:1096.
- [2] Jonas A, Legras R. *Polymer* 1991;32:2691.
- [3] Jones DP, Leach DC, Moore DR. *Polymer* 1985;26:1385.
- [4] Chen JY, Chen M, Chao SC. *Macromol Chem Phys* 1998;199:1623.
- [5] Chen M, Chen JY. *J Polym Sci Part B: Polym Phys* 1998;36:1335.
- [6] Chen M, Chung CT. *J Polym Sci Part B: Polym Phys* 1998;36:2393.
- [7] Chen M, Chung CT. *Polym Compos* 1998;19:689.
- [8] Velisaris CN, Seferis JC. *Polym Engng Sci* 1986;26:1574.
- [9] Day M, Deslandes Y, Roovers J, Suprunchuk T. *Polymer* 1991;32:1258.
- [10] Day M, Suprunchuk T, Cooney JD, Wiles DM. *J Appl Polym Sci* 1988;36:1097.
- [11] Hay JN, Kemmish DJ. *Plast Rub Proc Appl* 1989;11:29.
- [12] Bas C, Grillet AC, Thimon F, Alberola ND. *Eur Polym J* 1995;31:911.
- [13] Bas C, Battesti P, Alberola ND. *J Appl Polym Sci* 1994;53:1745.
- [14] Ko TY, Woo EM. *Polymer* 1996;37:1167.
- [15] Bassett DC, Olley RH. *Al Raheil IAM. Polymer* 1988;29:1745.
- [16] Cheng SZD, Cao MY, Wunderlich B. *Macromolecules* 1986;19:1868.
- [17] Ostberg GMK, Seferis JC. *J Appl Polym Sci* 1987;33:29.
- [18] Marand H, Prasad A. *Macromolecules* 1992;25:1731.
- [19] Blundell DJ. *Polymer* 1987;28:2248.
- [20] Lee Y, Porter RS. *Macromolecules* 1987;20:1336.
- [21] Lee Y, Porter RS, Lin JS. *Macromolecules* 1989;22:1756.
- [22] Marand H, Alizadeh A, Farmer R, Desai R, Velikov V. *Macromolecules* 2000;33:3392.
- [23] Tan S, Su A, Luo J, Zhou E. *Polymer* 1999;40:1223.
- [24] Lattimer MP, Hobbs JK, Hill MJ, Barham PJ. *Polymer* 1992;33:3971.
- [25] Lovinger AJ, Hudson SD, Davis DD. *Macromolecules* 1992;25:1752.
- [26] Verma R, Marand H, Hsiao B. *Macromolecules* 1996;29:7767.
- [27] Verma RK, Velikov V, Kander RG, Marand H, Chu B, Hsiao BS. *Polymer* 1996;24:5357.
- [28] Wang J, Alvarez M, Zhang W, Wu Z, Li Y, Chu B. *Macromolecules* 1992;25:6943.
- [29] Krüger KN, Zachmann HG. *Macromolecules* 1993;26:5202.
- [30] Hsiao BS, Gardner KCH, Wu DQ, Chu B. *Polymer* 1993;34:3986.
- [31] Hsiao BS, Gardner KCH, Wu DQ, Chu B. *Polymer* 1993;34:3996.
- [32] Tan SS, Su AH, Luo J, Zhou EL. *Polymer* 1999;40:1223.
- [33] Wang ZG, Wang XH, Hsiao BS, Phillips RA, Medellin-Rodriguez FJ, Srinivas S, Wang H, Han CC. *J Polym Sci Part B: Polym Phys* 2001;39:2982.
- [34] Liu T, Yan S, Bonnet M, Lieberwirth I, Rogausch KD, Petermann J. *J Mater Sci* 2000;35:5047.
- [35] Chung JS, Cebe P. *Polymer* 1992;33:2325.
- [36] Al Raheil IAM. *Polym Int* 1994;35:189.
- [37] Kim HG, Robertson RE. *J Polym Sci Part B: Polym Phys* 1998;36:1757.
- [38] Yoo ES, Im SS. *J Polym Sci Part B: Polym Phys* 1999;37:1357.
- [39] Wurm A, Merzlyakov M, Schick C. *Colloid Polym Sci* 1998;276:289.
- [40] Wurm A, Merzlyakov M, Schick C. *J Macromol Sci Phys* 1999;B38:693.
- [41] Pyda M, Wunderlich B. *J Polym Sci Part B: Polym Phys* 2000;38:622.
- [42] Goderis B, Reynaers H, Scherrenberg R, Mathot VBF, Koch MHJ. *Macromolecules* 2001;34:1779.
- [43] Jonas A, Legras R, Issi JP. *Polymer* 1991;32:3364.
- [44] Blundell DJ, Osborn BN. *Polymer* 1983;24:953.
- [45] TA Instruments. DSC 2910 differential scanning calorimeter, Operator's manual, Rev.8. New Castle, Delaware; 1997. p. C-73.
- [46] Reading M, Luget A, Wilson R. *Thermochim Acta* 1994;238:295.
- [47] Deslandes Y, Day M, Sabir NF, Suprunchuk T. *Polym Compos* 1989;10:360.
- [48] Hull D, Clyne TW. *An introduction to composite materials*, 2nd ed. Cambridge: University Press; 1996. p. 41.
- [49] Wei CL. Master Thesis, National Sun Yat-sen University, Kaohsiung, Taiwan; 2001.
- [50] Sauer BB, Kampert WG, Neal Blanchard E, Threefoot SA, Hsiao BS. *Polymer* 2000;41:1099.
- [51] Wang ZG, Hsiao BS, Sauer BB, Kampert WG. *Polymer* 1999;40:4615.
- [52] Wang Y, Lu J. *Polym J* 2000;32:560.